estimate single scattering albedos of 0.98 and 0.995, respectively, for the flights of these two dates. For the tropospheric samples, the integrating nephelometer aboard the B-23 was usually off-scale and above 10^{-3} m^{-1}. A typical value of σ_{ap} of 5×10^{-6} thus implies a lower limit for single scatter albedo of 0.995.

J. A. OGREN
R. J. CHARLSON
Department of Civil Engineering, University of Washington, Seattle 98195

L. F. RADKE
S. K. DOMONKOS
Department of Atmospheric Sciences, University of Washington

References and Notes

1. R. J. Charlson and M. J. Pilat, *J. Appl. Meteorol.* **8**, 1001 (1969).
2. J. M. Mitchell, *ibid* **10**, 703 (1971).
3. R. A. Reck, *Atmos. Environ.* **10**, 611 (1976).
4. J. B. Pollack, O. B. Toon, C. Sagan, A. Summers, B. Baldwin, W. Van Camp, *J. Geophys. Res.* **81**, 1071 (1976).
5. R. E. Newell, *Nature (London)* **227**, 697 (1970).
6. P. V. Hobbs, L. F. Radke, M. W. Eltgroth, D. A. Hegg, *Science*, **211**, 816 (1981).
7. J. B. Pollack, *ibid.*, p. 815.
8. J. A. Ogren, N. C. Ahlquist, A. D. Clarke, R. J. Charlson, *Geophys. Res. Lett.*, in press.
9. C. Lin, M. Baker, R. J. Charlson, *Appl. Optics* **12**, 1356 (1973).
10. R. E. Weiss, A. P. Waggoner, R. J. Charlson, D. L. Thorsell, J. S. Hall, L. A. Riley, *Proceedings of the Conference on Carbonaceous Particles in the Atmosphere* (*CONF-7803101*, Berkeley, Calif., 1979), pp. 257–262.
11. R. E. Weiss, thesis, University of Washington (1980).
12. M. Sadler, R. J. Charlson, H. Rosen, T. Novakov, *Atmos. Environ.*, in press.
13. N. H. Farlow, personal communication.
14. R. L. Chuan, personal communication. Size distributions were averaged over the period of sampling with the opal glass impactor.
15. These Mie computations of σ_{sp} from Ensor and Pilat (*16*) assume homogeneous spheres of H_2SO_4, a specific gravity of 1.8, and refractive index of $1.5 - 0i$, for a wavelength of 550 nm. Additional support for these calculations is provided by satellite measurements of stratospheric extinction, which were in the range 10^{-5} to 10^{-6} m^{-1} at a wavelength of 1 μm (M. P. McCormick, personal communication).
16. D. S. Ensor and M. J. Pilat, *J. Air Pollut. Control Assoc.* **21**, 496 (1971).
17. We thank N. C. Ahlquist for designing and building the optical measurement system. Supported in part by the NASA aerosol project under grand NSG-2362 and by NSF grant DPT 79-20857.

18 September 1980; revised 15 December 1980

Measurements of the Imaginary Part of the Refractive Index Between 300 and 700 Nanometers for Mount St. Helens Ash

Abstract. *The absorption properties, expressed as a wavelength-dependent imaginary index of refraction, of the Mount St. Helens ash from the 18 May 1980 eruption were measured between 300 and 700 nanometers by diffuse reflectance techniques. The measurements were made for both surface and stratospheric samples. The stratospheric samples show imaginary index values that decrease from approximately 0.01 to 0.02 at 300 nanometers to about 0.0015 at 700 nanometers. The surface samples show less wavelength variation in imaginary refractive index over this spectral range.*

The 18 May 1980 eruption of Mount St. Helens injected material into the stratosphere to an altitude of approximately 20 km, and the resulting stratospheric plume has covered major portions of the Northern Hemisphere (*1*). The possible effects on climate of this or of other volcanic injection of material into the stratosphere are determined by the radiative properties of the stratospheric aerosol.

In general these aerosol particles interact with solar and with thermal infrared radiation fields to produce temperature changes, both at the surface and at different levels in the atmosphere. The radiative effects of the aerosol depend on the optical constants of the aerosol and may be quite different for aerosols with differing optical constants.

These stratospheric aerosols are of two general types: a silicate ash produced directly at the time of the explosion and a sulfuric acid-water sulfate aerosol produced as a result of gas-to-particle conversion processes that occur in the volcanic plume. The silicate aerosol has its greatest relative importance in the months immediately after an eruption, while the sulfate aerosol is of relatively greater importance in later months.

Quantitative models that describe the radiative or climatic effects of these aerosols have been discussed by several investigators (*2-5*). In these models, the optical effects are based on numerical calculations in which it is assumed that the particles are homogeneous spheres. Scattering coefficients for Mie's solution for scattering of electromagnetic waves (*6*) are related to the size and composition of the particles through a size parameter $x = 2\pi r/\lambda$, where r is the particle radius and λ is the wavelength of the incident radiation, and a complex index of refraction $m = n_{RE} - i\, n_{IM}$, where the real part n_{RE} is the ratio of the speed of light in a vacuum to its speed in the particle, and the imaginary part n_{IM} is an absorption parameter that is related to the usual Bouguer-Lambert absorption coefficient k by means of the equation

$$n_{IM} = k\lambda/4\pi \qquad (1)$$

At visible wavelengths, both scattering and absorption are significant, as are details of the way in which solar energy is redistributed in the atmosphere because of particle scattering. At infrared wavelengths the optical effects are dominated by the absorption and emission characteristics of the aerosol, and the scattering behavior is of less importance.

The incident solar radiation that is scattered by the particles in the hemisphere away from the earth's surface may, as a first approximation, be considered to be lost to space. This effect acts to increase the planetary albedo, while the portion of the light scattered in the downward direction can still enter into the radiation balance of the earth-atmosphere system below the aerosol layer. The incident radiation that is absorbed in the layer by the particles also acts to decrease the planetary albedo. The relative contributions of each of the competing effects of the visible radiation lost to space by scattering and that retained by particle absorption have important consequences for the radiative effects of these particles.

Calculations of Coakley and Grams (*2*) suggest that particles in the size range of 0.1 to 1 μm have a net cooling effect on the earth's surface; the cooling effects due to the interaction of the aerosol with solar radiation are of greater magnitude than the heating due to infrared effects. The net cooling calculated depends on both the visible and the infrared optical constants of the aerosol as well as the size of the particles. Data of Pollack *et al.* (*5*) suggest a net cooling for the sulfuric acid aerosol but, depending on the actual optical constants, either heating or cooling is possible for the silicate aerosol.

In addition, calculations of rates of in situ heating induced by stratospheric aerosol particles are extremely sensitive to n_{IM} values at visible wavelengths. Fiocco, Grams, and Mugnai (*4*) calculated stratospheric heating rates as a function of latitude and of the albedo of the underlying earth-atmosphere system for four different models of the spectral variation in the complex index of refraction. They found that the rates of stratospheric heating induced by the aerosol layer are most sensitive to changes in the visible values of n_{IM}.

Both the visible and the infrared optical constants of the sulfuric acid-water

0036-8075/81/0220-0836$00.50/0

aerosol have been measured by Palmer and Williams (*7*); in particular, this sulfate aerosol will have a very low value of the n_{IM} ($< 10^{-7}$) at visible wavelengths. The silicate ash may be considered to be a much more heterogeneous component of the aerosol than the sulfate. Infrared measurements show, however, that the 10-μm silicate absorption feature that dominates the mid-infrared absorption spectrum of the volcanic ash has only a minor variation among samples ranging from basaltic to rhyolytic in composition (*8*).

Furthermore, quantitative measurements of the imaginary refractive index in this 10-μm region show that the values of n_{IM} for the silicate ash are similar to those of the sulfate aerosol. Since the modeling efforts discussed above suggest that the infrared optical properties are of less importance in determining the climatic effects of the aerosols than the visible optical properties, such differences in infrared absorption do not appear to be significant. The real refractive index of the silicate component of the aerosol is known to be approximately 1.5 to 1.6 through the visible. There is, however, a range of color associated with different samples of volcanic ash, from dark gray to nearly white, with corresponding differences in the measured imaginary refractive indices at visible wavelengths. It appears then that the uncertainty in the knowledge of the imaginary refractive indices at visible wavelengths is the major uncertainty associated with knowledge of the optical constants of the ash. Modeling of the radiative effects of the particular volcano such as Mount St. Helens requires knowledge of the absorptive properties of the ash at visible wavelengths.

Absorption measurements on the ash from the 18 May Mount St. Helens eruption were made for samples from several surface locations, including sites relatively close to the volcano in eastern Washington and more distant sites in Montana and Colorado, as well as for samples collected within the stratosphere at altitudes of 15 and 18 km.

Our surface samples could be separated into two groups on the basis of color: one was characterized by a pale gray appearance and the other by a somewhat darker gray appearance. These ash colors correspond to two major pulses of ash ejection by the volcano. The first pulse was reported to be dark gray, changing to a pale gray ash at approximately 1917 Universal Time (*1*). Trajectory analysis indicates that these surface samples represent material that was transported into the mid- to upper troposphere. Our stratospheric samples had, by comparison, a tan appearance, reflecting the size-fractionation of material that occurred with increasing altitude.

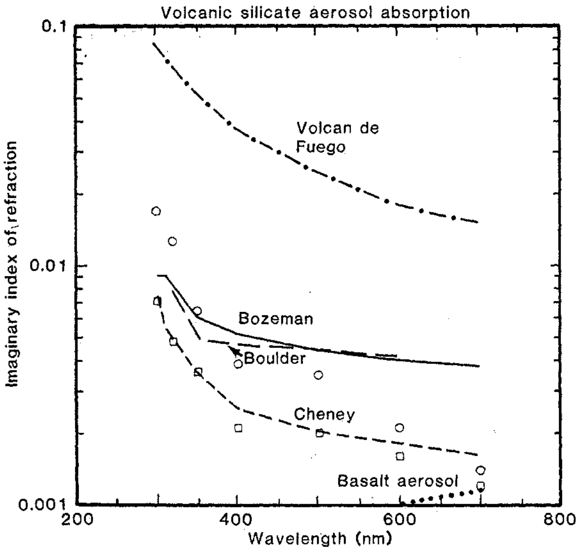

Fig. 1. Imaginary index of refraction measurements at visible wavelengths for three surface samples (Bozeman, Montana; Boulder, Colorado; Cheney, Washington) and two samples from the stratosphere (□, a 15-km sample from 20 May; ○, an 18-km sample from 21 May) of Mount St. Helens ash. A surface sample of ash from Volcan de Fuego and basalt data from (*5*) are also shown.

Surface samples were collected from ashfall material deposited on clean surfaces. Stratospheric samples were collected on IPC filters aboard an MB-57F aircraft flown in the lower stratosphere by NASA for the Los Alamos Scientific Laboratory. After an H_2O leach of soluble material, the samples were ashed to destruct the filter. Tests of samples of volcanic ash collected at the surface showed that this ashing procedure did not affect the measured absorption.

The absorption measurements were made by an integrating sphere technique with analysis by the Kubelka-Munk theory. The application of this technique to aerosol absorption measurements has been discussed by Patterson *et al.* (*9*) and by Lindberg and Laud (*10*). In general, the Kubelka-Munk theory is a phenomenological theory that relates the total diffuse reflectance R_∞ of a sample and the absorption-to-scattering ratio of the material.

In my procedure, total diffuse reflectance of a white standard ($BaSO_4$) is measured, and then the reflectance of a highly dilute mixture of the aerosol sample with the white standard is measured. For such a dilute mixture, the scattering coefficient of the mixture is the scattering coefficient of the standard. The absorption coefficient of the aerosol is determined from the two reflectance measurements and the known relative volume of the aerosol; the imaginary index of refraction is calculated from Eq. 1.

The results of these absorption measurements for the two gray samples from Bozeman, Montana, and Boulder, Colorado, are shown in Fig 1. The coloration of the two samples was quite similar, and there is excellent agreement between the two sets of absorption measurements. The absorption of another surface sample, a pale gray sample from Cheney, Washington (Fig. 1), is lower than that of the gray samples by a factor of 2 throughout much of the visible spectrum.

The stratospheric samples, a 15-km sample from the 20 May flight and an 18-km sample from the 21 May flight show values of n_{IM} that are consistent with surface measurements, but with a somewhat greater wavelength variation in n_{IM}, as expected from the differences in observed coloration. The two stratospheric samples have quite similar n_{IM} values near 700 nm; the 18-km sample, however, shows a significantly higher absorption near 300 nm than the 15-km sample.

For comparison, n_{IM} data for two other volcanic materials are presented in Fig. 1: ash from Volcan de Fuego in Guatemala and a basalt sample measured by Pollack *et al.* (*11*). The Fuego ash, measured by the same diffuse reflectance technique, is much darker than the Mount St. Helens ash and has a slight brown coloration. The n_{IM} values of the Fuego ash are roughly an order of magnitude higher than those of Mount St. Helens, with a wavelength dependence that is similar to that of our stratospheric samples. The basalt data are lower and show a different wavelength dependence.

The samples from the stratosphere were representative of the silicate aerosol that is likely to have the greatest potential impact on climate. Each of the stratospheric samples has a similar low value of n_{IM} ($\sim 1.5 \times 10^{-3}$) at 700 nm; it increases to approximately 0.007 for the 15-km sample and to 0.02 for the 18-km samples at 300 nm. The measured n_{IM} values for the stratospheric samples are in the same range as those for the surface samples. The stratospheric samples, however, show a greater wavelength dependence than the surface samples.

In contrast, a highly absorbing anthropogenic aerosol, elemental carbon, has an n_{IM} value of $\sim$ 0.6 throughout the visible spectrum (*12*). A white substance such as ammonium sulfate has an n_{IM} value of $< 10^{-7}$ (*13*) in the visible, and representative light tan desert aerosols have n_{IM} values that range from $\sim$ 0.003 at 700 nm to $\sim$ 0.02 at 300 nm (*14*).

The volcanic material measured by Pollack *et al.* (*11*) has smaller values of n_{IM} throughout the visible spectrum; a synthetic aerosol modeled by Ivlev and Popova (*15*) that was used for stratospheric calculations has an n_{IM} value of 0.005 through the visible; this value is larger than the stratospheric values for the wavelengths greater than 380 nm, a wavelength range that encompasses > 90 percent of the extraterrestrial solar flux.

In the absence of more detailed calculations, the modeled effects of the Mount St. Helens ash might be expected to be intermediate between those of the basalt aerosol (*5*) and those of the Ivlev and Popova aerosol (*2*, *4*). In particular, some significant in situ stratospheric heating due to the absorption of solar radiation by the aerosol would be expected; for particles of the size range with the greatest stratospheric lifetime, a net surface cooling, though by an amount smaller than that modeled for basalt, would be expected.

E. M. PATTERSON
*School of Geophysical Sciences,
Georgia Institute of Technology,
Atlanta 30332*

References and Notes

1. *Eos* **61**, 555 (1980).
2. J. A. Coakley, Jr., and G. W. Grams, *J. Appl. Meteorol.* **15**, 679 (1976).
3. Harshvardan and R. D. Cess, *Tellus* **28**, 1 (1976).
4. G. Fiocco, G. W. Grams, A. Mugnai, in *Proceedings of the Symposium on Radiation in the Atmosphere*, H. J. Bolle, Ed. (Science Press, Princeton, N.J., 1977), p. 74.
5. J. B. Pollack, O. B. Toon, C. Sagan, A. Summers, B. Baldwin, W. Van Camp, *J. Geophys. Res.* **81**, 1071 (1976).
6. G. Mie, *Ann. Phys.* **25**, 377 (1908).
7. K. F. Palmer and D. Williams, *Appl. Opt.* **14**, 208 (1975).
8. E. M. Patterson, in *Second Conference on Atmospheric Radiation* (American Meteorological Society, Boston, 1975), p. 177.
9. E. M. Patterson, D. A. Gillette, B. H. Stockton, *J. Geophys. Res.* **82**, 3153 (1977).
10. J. D. Lindberg and L. S. Laude, *Appl. Opt.* **13**, 1023 (1974).
11. J. B. Pollack, O. B. Toon, B. N. Khare, *Icarus* **19**, 372 (1973).
12. J. T. Twitty and J. O. Weinman, *J. Appl. Meteorol.* **10**, 725 (1971).
13. O. B. Toon and J. B. Pollack, *J. Geophys. Res.* **81**, 5733 (1976).
14. E. M. Patterson, *ibid.*, in press.
15. L. S. Ivlev and S. I. Popova, *Izv. Acad. Sci. USSR Atmos. Oceanic Phys.* **9**, 1034 (1973).
16. I thank N. Laulainen, D. Smith, T. Ackerman, and J. DeLuisi for providing the surface ash samples. I am especially indebted to W. Sedlacek for providing the stratospheric ash samples and the supporting data and measurements.

18 September 1980; revised 18 December 1980

Marine Macrophytes as a Global Carbon Sink

Abstract. *Marine macrophyte biomass production, burial, oxidation, calcium carbonate dissolution, and metabolically accelerated diffusion of carbon dioxide across the air-sea interface may combine to sequester at least 10^9 tons of carbon per year in the ocean. This carbon sink may partially account for discrepancies in extant global carbon budgets.*

Approximately 5×10^9 tons of carbon are released to the atmosphere annually as CO_2 by the burning of fossil fuel (*1*). Carbon dioxide remaining in the atmosphere accounts for about 50 percent of the fossil fuel carbon released; about 40 percent is estimated to diffuse across the air-sea interface into the dissolved CO_2 pool of surface ocean water (*2*-*4*). It has been suggested by default that increasing biomass on land accounts for the remaining 10 percent (*2*, *4*). An alternative argument is that there has been a net reduction of terrestrial biomass equivalent to 20 to 100 percent of the carbon liberated from fossil fuel (*3*, *5*, *6*).

Carbon sinks may fail to account for 0.5 to 5×10^9 tons of carbon per year. Substantial carbon sinks that have been overlooked or erroneous evaluation of

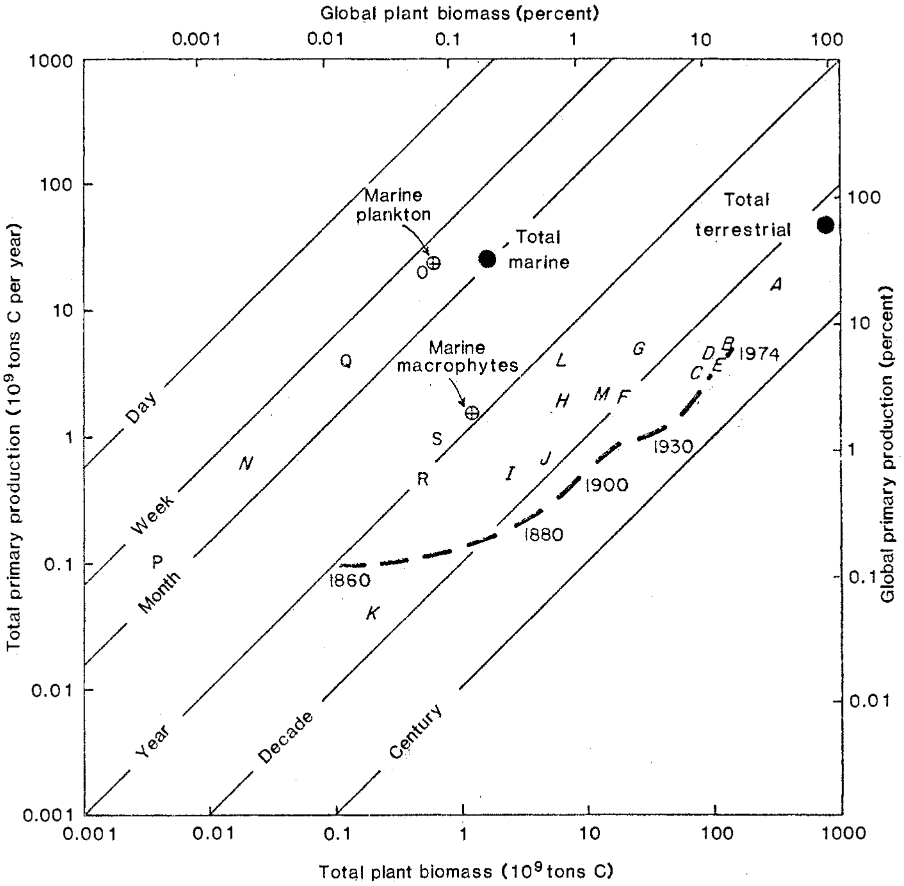

Fig. 1. Primary production, biomass, and turnover time for carbon in the biosphere, adapted from (*9*). Letters *A* to *N* (italic) indicate terrestrial ecosystems and remaining letters O to S (roman) indicate marine ecosystems: *A* is tropical rain forest; *B* is tropical seasonal forest; *C* is temperate evergreen forest; *D* is temperate deciduous forest; *E* is boreal forest; *F* is woodland and shrubland; *G* is savanna; *H* is temperate grassland; *I* is tundra and alpine meadow; *J* is desert scrub; *K* is rock, ice, and sand; *L* is cultivated land; *M* is swamp and marsh; *N* is lake and stream; O is open ocean; P is upwelling zones; Q is continental shelf; R is algal bed and reef; and S is estuaries. The cumulative fossil carbon input and the input rates (*1*) are shown as a dashed line. Since the source is not constant in size or input rate, the line represents a locus of points through time.